Seismic Intensity and Fourier Acceleration Spectra: Revised Relationship

Article *in* Earthquake Spectra · February 2002

DOI: 10.1193/1.1469037

1 author:

Vladimir Sokolov
Saudi Geological Survey
92 PUBLICATIONS **1,522** CITATIONS

Seismic Intensity and Fourier Acceleration Spectra: Revised Relationship

Vladimir Yu. Sokolov[a)]

This paper presents a revised method for estimating the seismic intensity (MMI or MSK scale) using Fourier amplitude spectra (FAS) of ground acceleration. The improvement of the recently proposed technique (Sokolov and Chernov 1998) has been made on the basis of the data, which were obtained recently during strong earthquakes that occurred throughout the world. The total amount of the used data (horizontal components of ground-motion recordings) is about 1,150 records, while the database of 300 recordings was used in the previous study. The method implies that the seismic intensity is determined by the level of ground motion spectral amplitudes in the frequency range of 0.4–13 Hz. The corresponding empirical relationships between FAS and each intensity level were developed. The method is validated by comparison of the results of the technique application with the empirical data, which have not been included in the database. The Romanian earthquakes (intermediate-depth events of 1977, 1986, and 1990) and the recent 1999 Hector Mine earthquake in southern California were used for this purpose. In general, the FAS intensity shows a good agreement with the reported intensity, and the average residuals do not exceed ± 0.3 intensity units and standard deviation is about 0.4-0.6. Evaluation of seismic intensity distribution using region- and site-dependent spectral models, as well as calculation of instrumental intensity map for the recent 1999 Chi-Chi earthquake, Taiwan, show that the FAS intensity clearly reflects the regional (source scaling and attenuation relation) and local (soil response) peculiarities of ground motion. [DOI: 10.1193/1.1469037]

INTRODUCTION

Seismic intensity (or severity of earthquake ground motion) is widely used throughout the world as a useful and simple quantity describing the damage due to earthquakes. The building codes, being in force in several countries, are based on the intensity values assigned to a given seismic region (Paz 1994), and seismic hazard maps are often constructed in terms of Modified Mercalli (MM) or Medvedev-Sponhauer-Karnik (MSK) intensity (e.g., Denham and Smith 1993, Dowrick et al. 1998, Schenk et al. 1996, Slejko et al. 1996). At the same time, intensity distribution patterns predicted for future destructive earthquakes are widely used for loss estimation (Shah et al. 1991, Corsanego 1995, Yong et al. 1996, Spence et al. 1998). With the density of seismic network in-

[a)] Geophysical Institute, Karlsruhe University, Hertzstr. 16, 76187 Karlsruhe, Germany

Earthquake Spectra, Volume 18, No. 1, pages 161–187, February 2002; © 2002, Earthquake Engineering Research Institute

creasing, it becomes possible to generate the intensity maps rapidly after an earthquake for public consumption via the World Wide Web (Wu et al. 1997; Wald et al. 1999a, b).

Many attempts have been made to correlate intensity with recorded ground motion parameters. The correlation of intensity with peak amplitudes (e.g., Trifunac and Brady 1975, Murphy and O'Brien 1977, Chernov and Sokolov 1983, Krinitzsky and Marcuson 1983, Aptikaev and Shebalin 1988, Chernov 1989, Spence et al. 1992, Wang 1995) shows typically large scatter. At present there is no doubt that seismic intensity is an expression of the amplitude, duration and frequency content of ground motion. Therefore, several attempts have been made to find relationship between intensity and combination of amplitude, period and duration (Chernov and Sokolov 1983), amplitudes of response spectra (Spence et al. 1992, Atkinson and Sonley 2000, Boatwright et al. 2001), or duration-dependent ground motion parameters, e.g., the "modified root of mean square of acceleration" (Wang 1995). The recent results obtained by Wald et al. (1999c) show that the MM intensity (I_{MM}) displays correlation with peak ground acceleration for the intensity range V$\leqslant I_{MM}\leqslant$VIII, and with peak ground velocity for V $\leqslant I_{MM}\leqslant$IX. These relationships are used for evaluation of instrumental seismic intensity in a real time seismographic system (Wald et al. 1999b). Thus, the frequency content of the motion is considered, even indirectly, but the duration is not taken into account. Spence et al. (1992) revealed that higher correlation between MM intensity and ground motion parameters are obtained when the 5% damping spectral acceleration (mean amplitudes in the short-period range 0.1–0.3 sec) is used instead of peak acceleration. Boatwright et al. (2001) showed that, for the 1994 Northridge, California, earthquake, correlations between the intensity and 5% damped pseudovelocity response spectra are strongest at 1.5 sec and weakest at 0.2 sec. Atkinson and Sonley (2000) developed empirical relationships between response spectra and MM intensity based on California earthquakes. The relationships were established for frequencies 0.5, 1, 2, 5, and 10 Hz and allow the estimate of spectral amplitudes from intensity values to within a factor of two.

The Fourier amplitude spectrum (FAS) does depend on the motion amplitude, duration and frequency content. The relations between FAS and MM intensity have been studied by Trifunac (1976, 1989), and Trifunac and Lee (1985, 1989). The empirical equations of FAS scaling in terms of MM intensity, local soil and geological conditions have been developed on the basis of records obtained in the western United States. These relations allow one to estimate the site-specific spectra using reported intensities. The technique to resolve the opposite problem—seismic intensity estimation using the Fourier amplitude spectrum of ground acceleration—has been proposed recently (Chernov 1989, Sokolov and Chernov 1998, Chernov and Sokolov 1999). The method implies that the intensity of earthquake ground motion (measured in terms of MM or MSK scales) can be determined by spectral amplitudes in a relatively narrow frequency band—so-called representative frequencies. The frequency band of 0.78-2.0 Hz is representative for $I_{MM}>$VIII, while 3–6 Hz range represents best I_{MM} V to VII, and the 7–8 Hz range correlates best with the lowest I_{MM}.

The collection of recordings obtained during recent earthquakes, which are accompanied by independent seismic intensity observations, allows the author to refine the re-

lationship between intensity and Fourier acceleration spectra. This paper presents the revised relationships and the technique of seismic intensity evaluation from the acceleration records.

DATA AND ANALYSIS

The data set that was used in the previous analyses (Chernov 1989, Sokolov and Chernov 1998, Chernov and Sokolov 1999) included horizontal components of 256 records obtained during main shocks and aftershocks of the following earthquakes: 1966 Tashkent (the USSR, central Asia); 1970 Dagestan (the USSR, Caucasus); 1971 San Fernando; 1976 and 1984 Gazli (the USSR, central Asia); 1976 Friuli (Italy); 1979 Imperial Valley; 1933–1968 western United States; and several earthquakes that occurred in the Caucasus and central Asia. The new database also includes the data from these earthquakes: 1983 Coalinga; 1984 Morgan Hill; 1986 North Palm Springs; 1987 Whittier Narrows; 1989 Loma Prieta; 1991 Sierra Madre; 1992 Cape Mendocino; 1992 Landers; and 1994 Northridge—all in California; 1992 Erzincan (Turkey); 1995 Hyogo-ken Nanbu (Kobe, Japan); and 1999 Izmit Bay (Turkey). When possible, the intensity point observations were correlated with the data from the nearest station (within 5–10 km), otherwise the intensity contour maps were used. The earthquake records and intensity data (partially) were obtained from World Wide Web sources (see, for example, http://pasadena.wr.usgs.gov/smdata.html, for a collection of the strong-motion data sources; http://www.ngdc.noaa.gov/seg/hazard/earthqk.shtml, for an earthquake intensity database). The intensity data for the Californian earthquakes were obtained from published sources (Bakun 1998, 1999) and from the U.S. Geological Survey (Dewey 1997). The intensities, in most cases, were estimated using MMI and MSK scales, which are essentially the same (see comparison in Sokolov and Chernov 1998). The JMA (Japanese Meteorological Agency) scale was used for the Hyogo-ken Nanbu earthquake, and the area of the location of the stations, recordings of which were used, was ranked as JMA VI (Irikura et al. 1996). The correspondent intensity MMI IX is assigned to these records (see comparisons of the MMI [MSK] and JMA scales in Murphy and O'Brien 1977, and Ohta et al. 1987). The strong-motion stations with assigned intensity of IX MMI (MSK) are listed in Table 1, and the records are shown in Figure 1.

It is necessary to note that the differences in earthquake parameters (magnitude, source mechanism, and distance), regional tectonics, propagation path properties, recording sites, and geological and geotechnical conditions are not taken into account. These factors are considered to be random variables affecting the ground motion parameters for a given intensity level.

The distribution of used data with respect to the levels of MMI (MSK) is as follows (the numbers of the records used in the previous study are shown in parentheses): MMI=III, 20 (20) records; MMI=IV, 80 (75) records; MMI=V, 326 (75) records; MMI=VI, 310 (45) records; MMI=VII, 303 (55) records; MMI=VIII, 116 (19) records; MMI=IX, 15 (6) records. Table 2 lists the earthquakes, records of which were obtained in the zones of intensity greater than MMI (MSK) VI.

Fourier amplitude spectrum of ground acceleration is used to study the relation between ground motion parameter and seismic intensity. To avoid confusion in terminol-

Table 1. List of strong-motion stations with assigned intensity of IX MMI (MSK)

Earthquake	Date	M	Country	Station code	Coordinates	Epicentral distance, km
Gazli	May 17, 1976	7.2	USSR	GZL	40.1N 63.28E	22
Erzincan	March 3, 1992	6.8	Turkey	ERC	39.754N 39.489E	13
Northridge	January 17, 1994	6.7	USA	LF6	34.132N 118.439W	13
				MOT	34.725N 135.28E	29
Hyogo-ken Nanbu (Kobe)	January 17, 1995	6.9	Japan	KBU	34.725N 135.24E	25
				PIS	34.67N 135.208E	20
Izmit Bay (Kocaeli)	August 17, 1999	7.7	Turkey	YPT	40.713N 29.783E	17
				SKR	40.737N 30.384E	34

ogy it is necessary to introduce some basic descriptions. The Fourier amplitude spectrum at frequency f is determined using standard Fourier series procedure (e.g., Bendat and Piersol 1980), as follows:

$$X(f)=\int_{-\infty}^{+\infty}x(t)\exp(-i2\pi ft)dt \tag{1}$$

$$X(f)=|X(f)|\exp(-i\Phi(f)) \tag{2}$$

where $X(f)$ is the Fourier transform of the time series $x(t)$, $|X(f)|$ is the amplitude spectrum and $\Phi(f)$ is the phase spectrum. Physically, the Fourier transform represents the distribution signal strength with frequency, that is, it is a density function, and sometimes it is called the *spectral density* (e.g., Savarenskii 1975). However, the term *spectral density* is also applied to the Fourier transform of the autocorrelation function (Bendat and Piersol 1980). Therefore, as a rule, the function $|X(f)|$ is called the *amplitude spectrum*. The finite range of Fourier transform is defined by

$$X(f,T)=\int_{0}^{T}x(t)\exp(-i2\pi ft)dt \tag{3}$$

where $X(f,T)$ is the Fourier transform of the time series $x(t)$ determined in the range $(0,T)$. The discrete version of Equation 3 is

$$X(f,T)=\Delta t\sum_{n=1}^{N}x_n\exp[-i2\pi fn\Delta t] \tag{4}$$

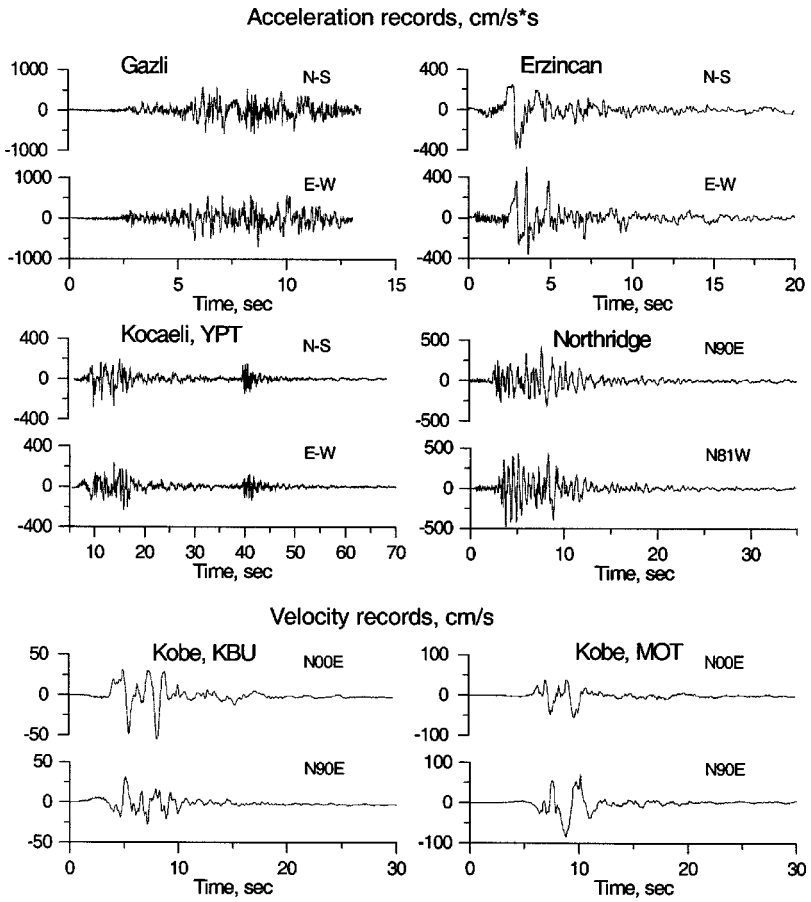

Figure 1. Examples of ground-motion recordings that were obtained at stations with assigned intensity of IX MMI (MSK).

or

$$X_k = X(k\Delta f) = \Delta t \sum_{n=1}^{N} x_n \exp[-i2\pi kn/N],$$

$$k = 1,2,...,N \tag{5}$$

where Δt is the sampling interval; N is the number of equally spaced points; Δf is the frequency interval ($\Delta f = 1/N\Delta t$). When x is measured in cm/s^2 (ground acceleration), the dimension of X_k is cm/s, etc. Thus, for the case of acceleration recordings, the function $|X(f)|$ is called below the Fourier acceleration spectrum or FAS and it is referred to as $A(f)$. The Fourier transform is characterized by the additive property: the Fourier transform (X_N) of a sum of time functions is the sum of their Fourier transforms ($X_1, X_2, ..., X_N$). However, it does not mean that the amplitude spectrum $|X_N|$ of a sum of

Table 2. Data retrieved from earthquakes

Earthquake	Magnitude	Number of records (horizontal components) for different intensities		
		VII	VIII	IX
Cape Mendocino, 1992	7.0	10	10	-
Coalinga, 1983	6.5	28	2	-
Erzincan (Turkey), 1992	6.8	-	-	2
Friuli (Italy), 1976	6.5	6	-	-
Gazli (USSR), 1976	7.2	2	-	2
Hyogo-ken Nanbu (Kobe), 1995	6.9	-	2	6
Imperial Valley, 1979	6.4	16	6	-
Izmit Bay (Kocaeli), 1999	7.8	16	7	3
Landers, 1992	7.3	6	4	-
Loma Prieta, 1989	7.0	62	15	-
Morgan Hill, 1984	6.1	6	4	-
North Palm Springs, 1986	6.2	9	-	-
Northridge, 1994	6.7	54	48	2
Spitak (Armenia), 1988	6.9	-	2	-
Whittier Narrows, 1987	6.1	40	2	-
western U.S. earthquakes, 1933–1968	5.6–6.7	12	14	-

time functions is the sum of their amplitude spectra ($|X_1|,|X_2|,...,|X_N|$). For example, it has been shown by Joyner and Boore (1986) that the summed radiation amplitude of N stochastic time functions increases as $\sqrt{N}$.

The Fourier amplitude spectra are widely used by seismologists to analyze earthquake source and path propagation properties. At the same time, in the case of frequency-dependent ground-motion parameters, the influence of local soil conditions may be easily considered using transfer (amplification) functions. The functions may be applied directly to modify the Fourier amplitude spectra. Engineers, however, are more familiar with another frequency-dependent characteristic of ground motion, the response spectra. Therefore, several researchers used the response spectra when analyzing relationship between seismic intensity and ground motion parameters. The response spectrum describes the maximum response of a single-degree-of-freedom (SDOF) system to a particular input motion as a function of the frequency and damping ratio of the SDOF system. Actually, the question of what type of spectrum—the Fourier amplitude spectrum or the response spectrum—can better describe the relationship between seismic intensity and ground motion is still open. The example below illustrates one of the advantages of using the Fourier spectrum.

The duration of strong ground motion can have a strong influence on earthquake damage. On the one hand, the duration is related to the time required for release of accumulated strain energy by rupture along the earthquake source. As a result, the duration of strong ground motion increases with increasing earthquake magnitude. On the other hand, the duration is affected by peculiarities of propagation path, regional geologic and

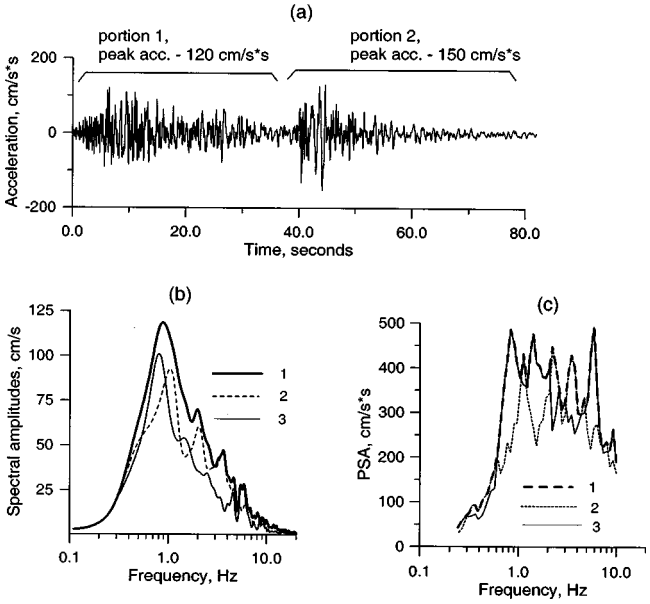

Figure 2. Illustration of influence of ground motion duration on the Fourier amplitude spectrum and the response spectrum: (a) N-S component of acceleration record, station Calitri, the M_S=6.9 Campano Luciano (Italy) (23 November 1980) earthquake; (b) Fourier amplitude spectra of the whole record (1), the first portion (2) and the second portion (3); (c) response spectra (5% damped).

local soil characteristics. Thus, the increase of duration is caused by frequency-dependent influence of various strong motion pulses. Obviously, the Fourier spectrum and the response spectrum reflect the influence. In some cases, earthquakes are treated as several separated events, and the recordings are composed of separate strong motion portions. The M_S=6.9 Campano Luciano (Italy) (23 November 1980) earthquake may be considered, among others, as an example of a double event. Figure 2a shows N-S component of acceleration record (Ambraseys et al. 2000) obtained in epicentral area (station Calitri, epicentral distance 16 km). Fourier amplitude spectra (smoothed) of the separate portions and the whole record are shown in Figure 2b and response spectra (5% damped) are shown in Figure 2c. The response spectrum for the whole record is an envelope of the response spectra of the two consecutive portions. At the same time, the amplitudes of Fourier spectrum calculated for the whole record $|X_{12}|$ are higher than the spectral amplitudes of the portions ($|X_1|$ and $|X_2|$). The average ratio $X_{12}|/(|X_1|+|X_2|)$ determined in the frequency range 0.2–15 Hz is about 0.71 that is almost equal to $1/\sqrt{2}$. Thus, the Fourier amplitude spectrum, in contrast to the response spectrum, provides direct account for ground motion duration. The results of comparison between reported intensity and values calculated using the Fourier spectra are described below.

When processing the ground motion data for the analysis in this study, the Fourier acceleration spectra $A(f)$ were calculated in the frequency range 0.2–17 Hz for the most significant portion of the horizontal components of the records and have been equally

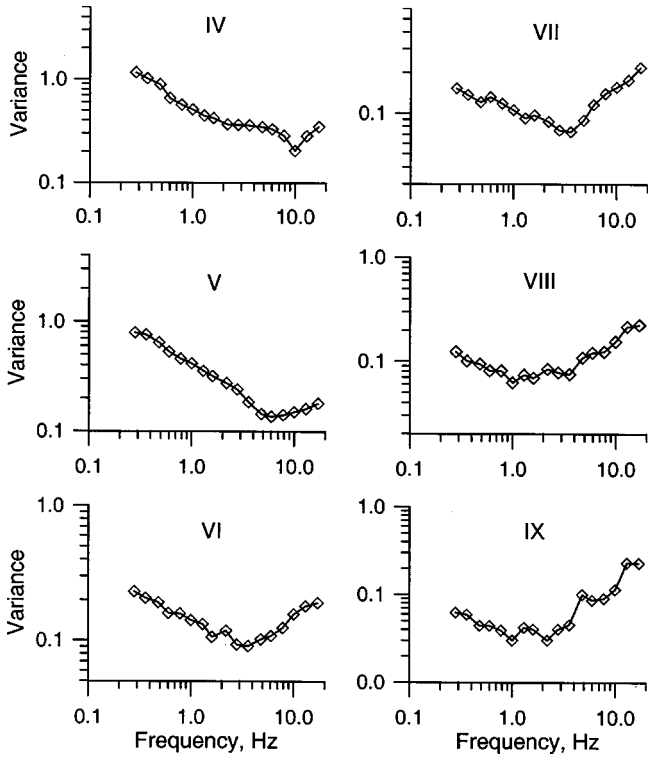

Figure 3. Variances (σ^2) of the values of $\log_{10} A$ versus frequency for different intensities MMI (MSK) IV–IX.

spaced in intervals of 0.1 $\log_{10}$ units. The variances (σ^2) of $\log_{10} A$ distribution with respect to the frequency are shown in Figure 3. The characteristics of the spectral amplitude distribution are not the same at different frequencies. The variances decrease within the frequency bands, which move to lower frequencies with increasing intensity. It is reasonable to suggest that the contribution of ground motion components to the ground motion severity is not the same at different frequencies. It is supposed that the variances of $\log_{10} A$ values are the least at the frequencies ($f_{\mathbf{R}}$) that are most "representative" for a given intensity.

The spectral components at five frequencies that are characterized by the smallest variance of $\log_{10} A$ have been selected for every considered intensity value (IV-IX), and the correlations between the values of $\log_{10} A$ and the levels of intensity I were studied considering all possible combinations of frequencies and intensities. As a result, the linear regression $\log_{10} A = F(I,f)$, characterized by the largest correlation coefficient $R = 0.86$ is the following (Figure 4).

$$\log_{10} A_f = 0.49I - 2.0 \tag{6}$$

The values of $\log_{10} A_f$ in this correlation are determined at the "representative" frequencies f_{R}, which depend on the intensity, and decrease with increasing intensity level.

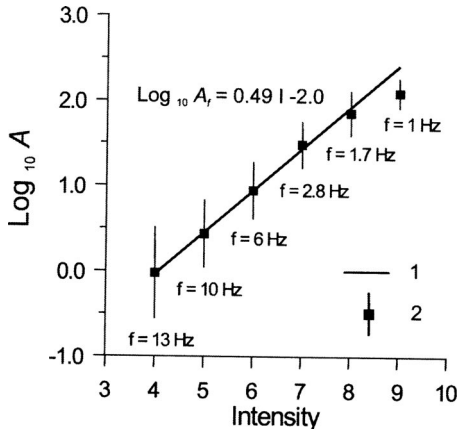

Figure 4. Fourier acceleration spectra/intensity relationship: 1—linear regression; 2—mean ± one standard deviation of the data.

It is necessary to note that the regression coefficients of the relationships (Equation 6) obtained in this study are similar with those determined previously (0.47 and -2.07, $R=0.92$, Sokolov and Chernov 1998) on the basis of the smaller amount of the data.

In previous papers (Sokolov and Chernov 1998, Chernov and Sokolov 1999), the simplest case was considered, assuming that a single frequency is "representative" for a given seismic intensity. In reality, the intensity of ground shaking is determined by joint influence of the ground motion components at different frequencies, however the contributions of these components change with the frequency. To illustrate the relationships between "representative" (or most contributing) frequency ranges and the intensity, let us consider the frequencies that are characterized by the values of standard deviation $\sigma_{1.3} \leqslant 1.3\sigma_{\min}$ (the $1.3\sigma_{\min}$ range is chosen as an example, and it represents the frequency range with the relatively large influence). Figure 5 shows the average spectra for different intensities and the parts of the spectra located within $\sigma_{1.3}$-area. The "representative" portions become wider (in terms of logarithm of frequency) and move to the low-frequency part of the spectra with increasing intensity.

The general idea of how to take into account the influence of different frequencies has been outlined previously (Chernov 1989, Sokolov and Chernov 1998) and, in this paper, the idea is realized to take into account the frequency range of engineering interest (0.3–14 Hz). The spectral amplitudes appear to be lognormally distributed (Figure 6). Thus, in order to estimate the intensity level I, it is necessary to calculate probability distribution function $F(i)=P[I \leqslant i]$, where i is the value of I in the range of interest.

Let us assume that an acceleration record has been obtained during an earthquake, and it is necessary to estimate the intensity level (instrumental intensity) at a site in terms of MMI (or MSK) scale. The random variable I will not exceed the given value i when the base 10 logarithm of the levels of acceleration spectrum ($\log_{10} A$) at the frequencies f_i that are considered as "representative" for this intensity level (i) will not exceed the certain values of $\log_{10} A_0$. The spectra (A_0) are the average spectral amplitudes

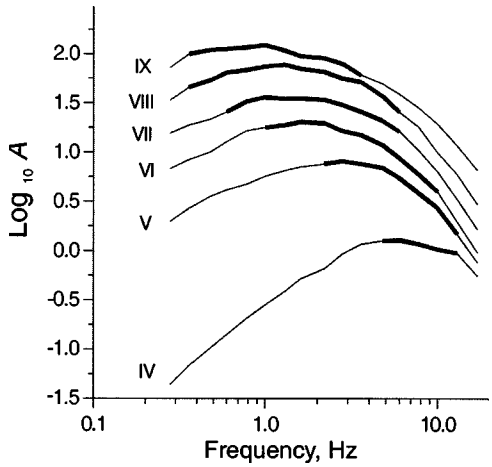

Figure 5. Mean acceleration spectra (cm/s) for different intensities (IV–IX MMI). Thick lines show spectral amplitudes located within area of $\sigma_{1.3} \leqslant 1.3\sigma_{\min}$ (see text).

for different intensities $I=i$ ("assigned spectra," Figure 5), and the "representativeness" of the spectral components depends on their variance (σ_f^2). Thus, the probability that the intensity level I at the recording site will not exceed the given value i may be estimated using the following scheme.

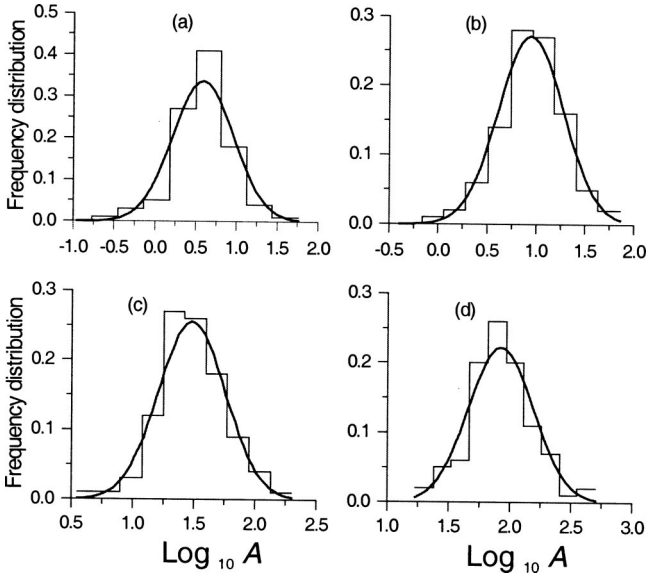

Figure 6. Distribution of $\log_{10} A$ values at certain frequencies for intensities V–VIII: (a) intensity V MMI, frequency 10 Hz; (b) intensity VI MMI, frequency 6 Hz; (c) intensity VII MMI, frequency 2.8 Hz; and (d) intensity VIII MMI, frequency 1.7 Hz.

The probability that the base 10 logarithm of the levels of Fourier acceleration spectra ($\log_{10} A$) at the frequency f_j will not exceed the values of $\log_{10} A_0$, which are assigned to this intensity level ($I=i$), is estimated as follows:

$$P[x_j \leqslant a_{i,j}] = 1 - 1/(\sigma_{i,j}\sqrt{2\pi}) \int_{x_{\min}}^{x_j} \exp(-[a_{i,j} - x_j])^{1/2}/(2\sigma_{i,j}^2) dx \quad (7)$$

where $a_{i,j}$ and $\sigma_{i,j}$ are the mean and the standard deviation of $\log_{10} A_0$ at the frequency f_j assigned to the intensity $I=i$; x_j is the base 10 logarithm of the level of observed spectrum at frequency f_j; $x_{\min}$ is determined as $x_{\min} = a_{i,j} - 5\sigma_{i,j}$. To take into account the influence of all considered frequencies, the probability $P[x_j \leqslant a_{i,j}]$ is calculated for every frequency, and the resulting probability $P[x \leqslant a_i]$ for the intensity i is obtained as

$$P[x \leqslant a_i] = \left(\sum_{j=1}^{j=n_f} [x_j \leqslant a_{i,j}] w_{i,j} \right) \Big/ \sum_{j=1}^{j=n_f} w_{i,j} \quad (8)$$

where n_f is the number of considered frequencies; $w_{i,j}$ is the weight, which depends on the variance $\sigma_{i,j}^2$. The value of $w_{i,j}$ is calculated as $w_{i,j} = \sigma_{i,\min}^2 / \sigma_{i,j}^2$, where $\sigma_{i,\min}^2$ is the minimum variance for the intensity i. Obviously, when considering the condition of intensity $I=i$ not to be exceeded, it is necessary to take into account the larger intensities $I>i$. Therefore, the probability that the intensity level I at the recording site will not exceed the given value i may be estimated as follows:

$$P[I \leqslant i] = \prod_{i}^{i=12} P[x \leqslant a_i] \quad (9)$$

The desired value of instrumental intensity is estimated by the maximum of the first derivative of function P (Figure 7). In practice the frequency range from 0.36 Hz to 13 Hz is considered, because, as a rule, the frequencies that lie outside this range are filtered during the data processing. The spectral amplitudes, which should be assigned to intensities III and X–XII, were obtained by simple extrapolation from the nearest intensities (IV–V and VIII–IX). Tables 3 and 4 list the characteristic parameters of the model.

MODEL VALIDATION

To validate the technique it is necessary to compare the results of the technique application with the empirical data, which have not been included into the database. First, let us consider the example shown in Figure 2a: the acceleration record obtained during the $M_S = 6.9$ Campano Luciano (Italy) (23 November 1980) earthquake in epicentral area (station Calitri, epicentral distance 16 km). The reported intensity value for the site is about VIII+-IX MCS (Mercalli, Cancani, Sieberg) scale (the intensity database of damaging earthquakes in the Italian area, see http://emidius.itim.mi.cnr.it/DOM/home.html). The correspondent intensity MMI VIII may be assigned to the record (see comparisons of the MMI and MCS scales in Murphy and O'Brien, 1977). The calculated intensity values (averaged from two horizontal components) are as follows: portion 1—7.2; portion 2—7.3; whole record—8.1. Thus, the instrumental intensity determined on the basis of Fourier acceleration spectrum allows taking into account the influence of

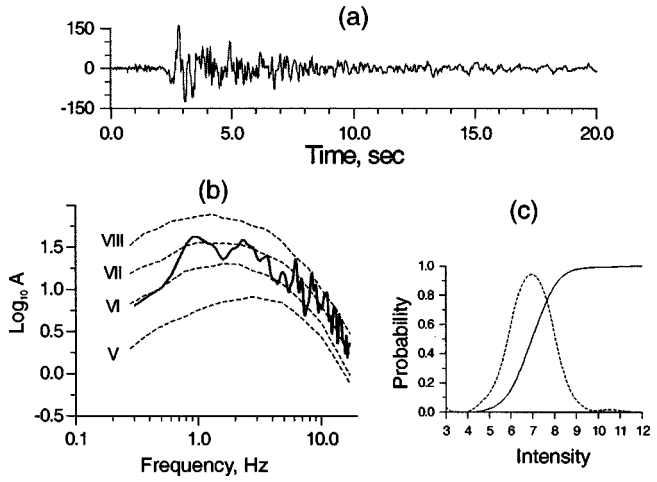

Figure 7. Seismic intensity estimation on the basis of Fourier acceleration spectrum: the case of the 1977 (M=7.4, H=100 km) Vrancea earthquake, station Incerc (Bucharest). (a) Acceleration record (cm/sec^2), E-W component; (b) comparison of the spectrum of real record (solid line, E-W component) and the mean spectra (dashed lines) for various intensities (V–VIII); and (c) probability function of intensity not to be exceeded (solid line) and first derivative of the function (dashed line).

Table 3. Characteristics of the empirical model (mean acceleration spectra, $\log_{10}$ A) used for evaluation of seismic intensity from the Fourier amplitude spectra

	Intensity							
Freq., Hz	3	4	5	6	7	8	9	10
0.36	−1.97	−1.17	0.43	0.92	1.27	1.66	2.0	2.2
0.48	−1.74	−0.99	0.55	1.0	1.33	1.73	2.04	2.25
0.6	−1.55	−0.85	0.62	1.1	1.41	1.81	2.05	2.3
0.78	−1.35	−0.69	0.67	1.21	1.51	1.84	2.07	2.45
1.0	−1.15	−0.55	0.75	1.25	1.56	1.87	2.09	2.35
1.3	−1	−0.41	0.81	1.28	1.54	1.89	2.03	2.3
1.68	−0.8	−0.28	0.85	1.31	1.55	1.85	1.98	2.25
2.2	−0.68	−0.18	0.88	1.29	1.54	1.82	1.96	2.15
2.8	−0.5	−0.03	0.91	1.22	1.48	1.75	1.9	2.0
3.6	−0.38	0.07	0.88	1.18	1.4	1.72	1.78	1.88
4.8	−0.3	0.1	0.84	1.07	1.32	1.57	1.7	1.8
6.0	−0.32	0.11	0.74	0.94	1.21	1.4	1.6	1.7
7.8	−0.35	0.07	0.58	0.78	1.02	1.26	1.45	1.55
10.0	−0.4	0.01	0.43	0.6	0.8	1.0	1.29	1.39
13.0	−0.43	−0.03	0.17	0.3	0.53	0.78	1.07	1.17

Table 4. Characteristics of the empirical model (standard deviation of $\log_{10}$ A) used for evaluation of seismic intensity from the Fourier amplitude spectra

	Intensity							
Freq., Hz	3	4	5	6	7	8	9	10
0.36	1.0	1.0	0.87	0.45	0.37	0.32	0.24	0.24
0.48	0.94	0.94	0.8	0.44	0.35	0.31	0.22	0.22
0.6	0.8	0.8	0.73	0.4	0.36	0.28	0.21	0.21
0.78	0.75	0.75	0.68	0.4	0.34	0.28	0.2	0.2
1	0.71	0.71	0.64	0.38	0.33	0.25	0.17	0.17
1.3	0.67	0.67	0.59	0.36	0.3	0.27	0.17	0.17
1.68	0.65	0.65	0.56	0.33	0.31	0.26	0.17	0.17
2.2	0.61	0.61	0.52	0.34	0.29	0.27	0.17	0.17
2.8	0.6	0.6	0.49	0.3	0.27	0.28	0.2	0.2
3.6	0.6	0.6	0.43	0.3	0.27	0.29	0.21	0.21
4.8	0.59	0.59	0.38	0.32	0.3	0.33	0.29	0.29
6.0	0.57	0.57	0.37	0.33	0.34	0.35	0.29	0.29
7.8	0.53	0.53	0.38	0.35	0.37	0.36	0.3	0.3
10.0	0.45	0.45	0.39	0.4	0.39	0.39	0.34	0.34
13.0	0.53	0.53	0.4	0.42	0.42	0.44	0.46	0.46

consecutive strong motion pulses. The influence of regional (source scaling and attenuation relation) and local (soil response) peculiarities of ground motion on instrumental intensity will be discussed below.

THE VRANCEA (ROMANIA) REGION

In this section, the data obtained during the 1977 (M=7.4, H=100 km), the 1986 (M=7.1, H=130 km), and the 1990 (M=6.9, H=90 km) Vrancea (Romania) earthquakes (Oncescu et al. 1992, 1999) are considered. The shallow intraplate events produced the overwhelming part of the data used for developing the technique, therefore it is possible to evaluate the applicability of the method in the case of intermediate depth events. In this case, all necessary parameters of the model have been determined using the database, which does not include the records from these events. The intensity was evaluated from the earthquake records and compared with reported data—maps of seismic intensity distribution (Radu and Polonic 1979, Radu et al. 1987, Radu and Utale 1990). Table 5 lists the results of the comparison.

It is seen that the intensity values estimated by the spectra of the records (I_{ins}) are consistent with the reported intensities (I_{rep}). The intensity estimations for the stations, which are located on consolidated sediments or rock (Carcaliu, Iasi, Istrita, Muntele, Surduc, Vrincioia), constantly show the values that are less (more than 0.5 units of intensity) than the reported intensities. The empirical data, which are taken from generalized macroseismic maps, represent intensity distribution for so-called average soil condition. Therefore, the decreased values of estimated intensity for the rock-site stations, as compared with the empirical "average soil" data, reflect the general dependence of

Table 5. Comparison between reported and instrumental intensity values (calculated using the spectra of records) for earthquakes in the Vrancea (Romania) area

Station	Reported intensity	Instrumental intensity	
		N-S component	E-W component
	Earthquake of 1977, M=7.4, H=100 km		
Incerc (Bucharest)	VII-VIII	7.6	7.1
	Earthquake of 1986, M=7.2, H=133 km		
Bacau	VI-VII	6.4	6.5
Bucharest (Magurele)	VI-VII	6.9	6.6
Carcaliu*	VI	5.4	5.5
Carlton (Bucharest)	VI-VII	6.0	6.0
Cernavoda	VI	5.9	5.7
Eren (Bucharest)	VI-VII	6.5	6.6
Focsani	VIII	7.9	7.7
Iasi*	VII	6.0	6.0
Incerc (Bucharest)	VI–VII	6.4	6.4
Istrita*	VII	6.7	6.4
Militari (Bucharest)	VI-VII	6.3	6.3
Muntele*	VI-VII	5.8	5.2
Surduc*	VII	6.4	6.2
Vrincioia*	VII-VIII	6.4	6.9
	Earthquake of 1990 (May 30), M=6.9, H=90 km		
Bacau	VII	7.0	6.9
Carcaliu*	VI-VII	6.5	5.9
Cernavoda	VI	6.6	6.5
Iasi*	VII	6.3	6.2
Incerc (Bucharest)	VII	6.4	6.7
Muntele*	VI-VII	5.0	5.2
Panduri (Bucharest)	VII	6.6	6.5
Surduc*	VII	6.2	6.3
Vrincioia*	VII	6.4	6.8

*Consolidated sediments or rock sites.

intensity on the local site conditions. The averaged residuals between observed and calculated intensity values (model bias) are as follows: the case of reported "average soil" intensity—average residual 0.4, standard deviation 0.45; the reported intensity values were decreased by 1 unit for rock sites—average residual 0.05, standard deviation 0.37.

THE HECTOR MINE (CALIFORNIA) EARTHQUAKE

The independent macroseismic data (reported intensity) are also available for the recent Hector Mine earthquake (M 7.1, 16 October 1999, California). The Hector Mine earthquake occurred in an uninhabited region and only caused moderate shaking in sparsely populated parts of the Mojave Desert. There are two sources of independent macroseismic data: Community Intensity Map (Scientists from the U.S. Geological Survey et al. 2000) and the official U.S. Geological Survey assignments (Dewey 1997). The

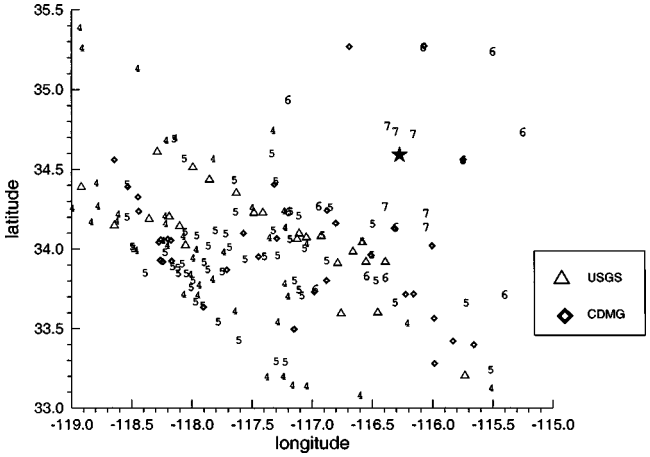

Figure 8. Observations for the 1999 Hector Mine event (a part of the total observational data set). The epicenter is plotted as black star. The strong-motion stations are shown as symbols, while the intensity values (Dewey 1997) are represented by numbers giving the reported MMI.

community map may be biased due to the large size of the zip code areas: the intensity values are effectively averaged, reducing the peak value. When compiling the map, a certain intensity value was assigned to the whole zip area. At the same time, there is no guarantee that the reported intensity will correspond with the intensity at the strong motion station, even if it is located within a few kilometers from the place of the intensity observation. Figure 8 shows the distribution (fragment) of the strong motion stations (CDMG—the California Division of Mines and Geology; USGS—the U.S. Geological Survey) recording of which are used for the instrumental intensity evaluation by peak amplitudes method and the MMI observation points (J. Dewey's data). It can be seen that in many cases the ground-motion stations are surrounded by intensity observations that differ by 1 MMI unit, and even 2 MMI units. Thus it is necessary to accept that the MMI value at the instrumental site can be determined to within an uncertainty of 1 MMI unit.

Table 6 presents a comparison between the U.S. Geological Survey-reported intensity and instrumental intensity evaluated from the records using the Fourier spectra. The ground motion records were obtained from URL=http://smdb.crustal.ucsb. The comparison is shown for ground-motion stations, which have the reported intensity values at distances less than 5 to 10 km. In general, the instrumental intensity (I_{ins}) values agree with the reported intensity (I_{rep}), and the difference between I_{ins} and I_{rep} does not exceed 1 MMI unit. The average MMI residual between observed and calculated intensity values (model bias) is -0.3 ± 0.63. In several cases, i.e., stations AMB, JST, and Morongo, the difference between observations and calculations is more than 1 MMI. The observed intensities may also differ by 2 MMI units within a few kilometers (see Figure 8, area within 116.8–117.5 W and 33.7–34.3 N). Most probably, the influence of local soil conditions may be the reason for the differences, but this assumption should be verified. For example, the records and spectra for AMB station reveal the presence of high-amplitude low-frequency (about 1 Hz) components, and the data for station BKR show high am-

Table 6. Comparison of observed intensity (Dewey 1997) and instrumental intensity estimated using Fourier amplitude spectra method (CDMG and USGS stations)

Owner	Station	Latitude	Longitude	Observed intensity (MMI)	Instrumental intensity (N-S and E-W component)	Soil condition*
CDMG	NWN	34.39	−118.53	V	4.3, 4.5	Q
-	MLK	33.92	−118.24	V	4.2, 4.5	
-	LUH	34.062	−118.198	IV	4.6, 4.8	Q
-	DOW	33.924	−118.167	V	4.3, 4.5	Q
-	NBI	33.634	−117.902	V	4.4, 4.6	Q
-	FYP	33.869	−117.709	V	4.2, 4.7	Q
-	RVA	33.951	−117.709	V	4.7, 4.8	Q
-	H4P	34.05	−117.311	V	5.4, 5.5	
-	H05	33.729	−116.979	VI	5.9, 5.7	Q
-	BBF	34.241	−116.872	VI	7.2, 6.6	
-	DSP	33.962	−116.509	V	6.3, 6.1	Q
-	JST	34.131	−116.314	VI	7.4, 7.3	Q
-	BKR	35.272	−116.066	VI	6.5, 7.2	Q
-	AMB	34.56	−115.743	VI	7.8, 7.5	Q
USGS	Fillmore	34.397	−118.918	IV	4.3, 4.3	D
-	Calabasis	34.155	−118.641	IV	4.3, 4.2	D
-	Paulette	34.21	−118.186	IV	4.4, 4.2	
-	Palmdale	34.15	−118.101	V	4.6, 5.3	CD
-	Whittier Narr.	34.032	−118.052	IV	4.8, 4.5	D
-	Littlerock	34.521	−117.99	V	5.4, 5.1	D
-	Wrightwood	34.36	−117.629	V	5.3, 5.4	BC
-	Mentone	34.07	−117.121	V	4.6, 4.9	
-	Seven Oaks	34.105	−117.105	V	5.4, 5.6	BC
-	Forest Falls	34.088	−116.921	V	5.4, 5.6	
-	Morongo	34.048	−116.578	V	6.5, 6.4	
-	N. Palm Spr.	33.925	−116.548	V	6.1, 6.0	D
-	Fun Valley	33.925	−116.389	VI	6.4, 6.5	

*CDMG stations—geology classification after Park and Elrick (1998); Q=Quaternary rock. USGS stations—NEHRP site classes (BSSC 1995), values taken from map of Wills et al. (2000).

plitudes in the frequency range of 1–3 Hz (Figure 9). The ground motion records obtained at these stations during the 1992 Landers earthquake also reveal the highest spectral amplitudes at the same frequencies as those observed during the Hector Mine earthquake (Figure 9).

It is obvious that the technique described above (as well as other relationships between macroseismic intensity and ground motion parameters) can be applied only for estimation and prediction of "average" intensity without consideration of the behavior of a particular structure. Therefore, one of the major applications of the technique is a compilation of a so-called instrumental intensity map showing the overall distribution of

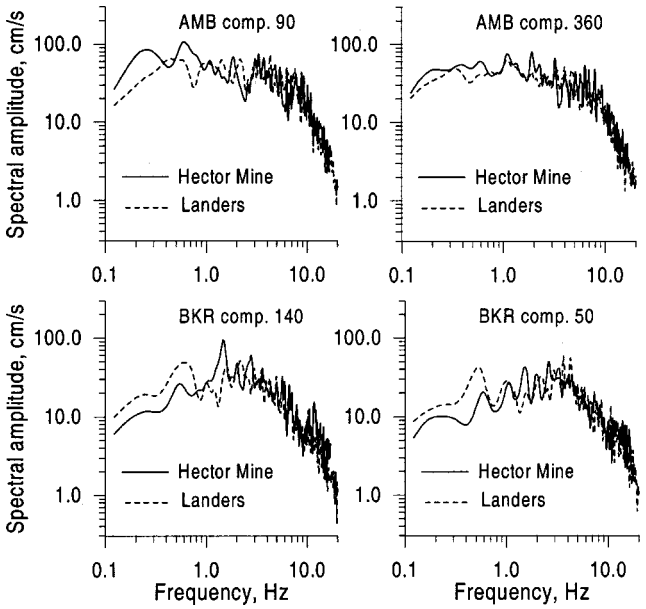

Figure 9. Comparison between spectra of ground acceleration registered during the Hector Mine and Landers earthquakes at stations AMB and BKR.

the intensity on the shaked territory. In regions of sparse station spacing, ground motion parameters to be used for the intensity calculation are estimated using magnitude-distance regressions and frequency- and intensity-dependent site correction factors (Wald et al. 1999a). Thus, a combined empirical-theoretical approach is used. In the case of the intensity/Fourier amplitude spectra relationship it is possible to use the regional spectral scaling and attenuation models, as well as the intensity-dependent spectral amplification functions describing the influence of local site conditions. To demonstrate the potential of the approach the theoretical isoseismals were calculated for the Hector Mine earthquake using a regional ω-square source-scaling model for California. There are three general spectral models developed for California earthquakes, namely the Brune single-corner frequency model, the two-corner frequency model, and the empirical regression model (see, for example, Atkinson and Silva 2000). However, for magnitude M=7 these three models produce nearly equivalent spectra for frequencies greater than 0.4 Hz. The spectra were calculated using a seismic moment value of 6.3 $\times 10^{26}$ dyne cm (Ji et al. 2002) and a stress parameter $\Delta\sigma$ that ranged from 20 to 80 bars. The attenuation was modeled by geometric spreading of R^{-1} to a distance of 40 km, with $R^{-0.5}$ spreading for R greater than 40 km. Here R is the distance to the nearest point of the source plane. The attenuation was modeled by geometric spreading of R^{-1} to a distance of 40 km, with $R^{-0.5}$ spreading for R greater than 40 km. Here R is the distance to the nearest point of the source plane. The anelastic attenuation was represented by a frequency-dependent regional quality factor given by $Q=180f^{0.45}$ (Raoof et al. 1999, Atkinson and Silva 2000). To take into account the site response factor, we used the generalized amplification function for so-called generic soil (Boore and Joyner

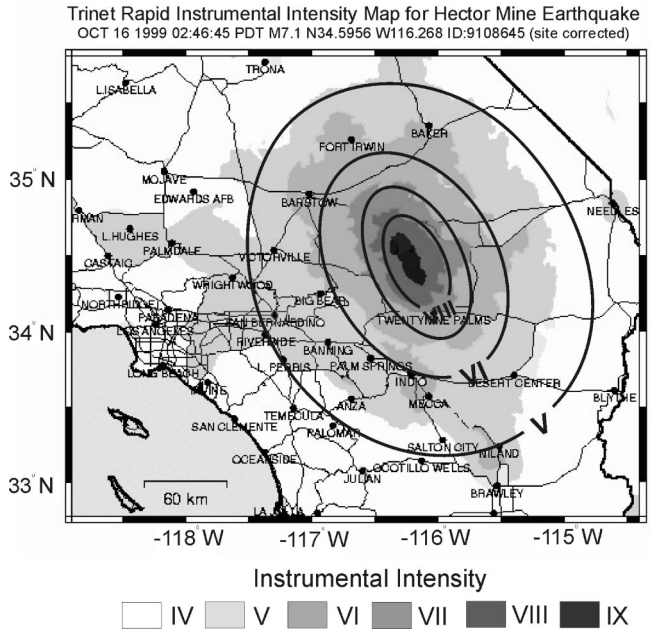

Figure 10. Comparison of theoretical isoseismals, which were calculated using regional- and site-specific spectral models (see text) and TriNet instrumental intensity map.

1997). The amplification function represents the influence of a soil column with an average shear-wave velocity of 310 m/sec for the upper 30 meters, and it corresponds to Soil Profile Type CD in the 1994 *NEHRP Provisions* (BSSC 1995).

Figure 10 shows comparison between the theoretical isoseismals (variant for stress parameters $\Delta\sigma$ of 30 bars) and instrumental intensity map calculated using the peak amplitude method. The agreement is quite good. The discrepancies may be explained by the influence of local site conditions. Our calculations show that, when using the generalized amplification function for the soil of NEHRP Class D, the theoretical intensities increase at 0.5-0.3 MMI units for intensities from VII to IV respectively. Obviously, when using the NEHRP Class E (soft soil) amplification function, the difference in intensity values with "generic soil" class should be larger.

To display the possibility of the technique to take into account the regional and local peculiarities of seismic ground motion, a comparison of the intensity attenuation curves for an earthquake of magnitude 7.0, which were calculated for two different regions: the western United States (California) and the eastern part of North America (ENA), is shown in Figure 11. The spectral models for these regions are characterized by different source scaling and attenuation relations (Boore and Atkinson 1987): for example, $Q = 180f^{0.45}$ for California earthquakes, and $Q = 680f^{0.36}$ for ENA earthquakes. Three models of local site condition are used, namely: rock and generic soil (Boore and Joyner 1997), and deep (thickness of 250-300 m) alluvium deposits. The curves clearly reflect

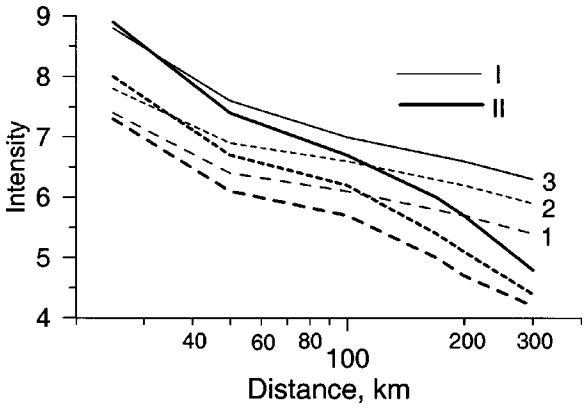

Figure 11. Intensity attenuation curves (M=7.0) evaluated using different spectral models (I—eastern North America, and II—the western United States [California]) and soil conditions (1—rock, 2—generic soil, and 3—deep alluvium deposits).

the differences in regional and local characteristics of ground motion. It is necessary to note that, in this case, the nonlinear behavior of soft soil during strong excitation has not been taken into account.

THE CHI-CHI, TAIWAN, EARTHQUAKE

A disastrous earthquake (M_W=7.6, M_L=7.3) occurred at 1:47am, local time on 21 September 1999 in Taiwan. It caused significant damage in the nearby areas of mid-Taiwan. About 10,000 buildings collapsed or were heavily damaged, and the death toll was more than 2,300 (Chen et al. 2000, Tsai et al. 2000). Taiwanese engineers do not use the macroseismic scale for describing earthquake damage, however the Seismological Center of the Central Weather Bureau (CWB) reported seismic intensity in terms of JMA scale in maps distributed after every earthquake. For the Chi-Chi main shock, the intensity was reported as VI JMA (MMI 9-10) for the epicentral area and IV JMA (MMI 6-7) for the Taipei city located more than 130 km north of the epicenter (see Figure 12). Faulting during the earthquake was interpreted as reverse, left-lateral faulting on a low-angle north-south trending plane (e.g., Furumura et al. 2000, Iwata et al. 2000, Lee and Ma 2000). The surface faulting along the Chelungpu fault produced by the earthquake (Figure 12) extends north-south about 96 km, and has a maximum horizontal slip of about 10 m and a maximum scarp height about 8 m (Lee et al. 2000). Figure 12 also shows locations of free-field, three-component, accelerograph stations (Taiwan Strong Motion Instrumentation Program [TSMIP]) recordings of which are used in this study. It is necessary to note that most of the stations to the west and south of the epicenter (CHY, KAU, and TCU arrays) are located in deep alluvium area of the Western Coastal Plain.

The Chi-Chi earthquake has been registered by many stations and it is possible to calculate "Instrumental Intensity" (II) map and to compare the map (Figure 13) with data reflecting the severity of seismic vibration, namely: the distribution of partially and completely collapsed buildings (see http://www.ncree.gov.tw) and fatality rate per

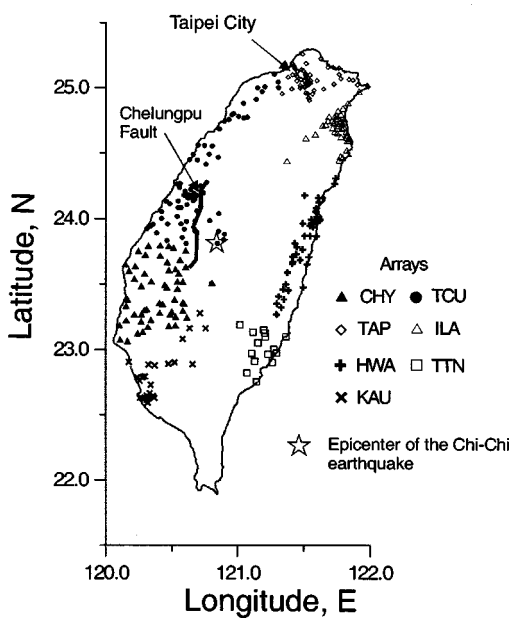

Figure 12. Location of epicenter of the M_W 7.6 Chi-Chi (Taiwan) earthquake, ruptured Chelungpu Fault and free-field digital accelerograph stations (TSMIP network).

10,000 residents (Y. B. Tsai, National Central University, Chung-Li). The zone of highest damage completely lies within the area outlined by isoseismal IX II. The areas of maximum assigned intensity (more than IX II) coincide with the areas of highest fatality rate.

The instrumental intensity isoseismals also reflect local geology. The distribution of intensity in the far-field zone shows the higher values on the areas covered by Quaternary sediments, namely, the western part of Taiwan (coastal plain), the northern part (Taiwan Basin and Ilan Plain), and the narrow and long area near the eastern coast (Longitudinal Valley). Although the Taipei basin is located more than 130 km away from the epicenter of the Chi-Chi earthquake, the level of damage in the area was greater than most counties in the northern region (Tsai et al. 2000). In the Taipei basin there were three tall buildings that collapsed and many (about 480) low-rise structures were damaged during the earthquake. The instrumental intensity maps exhibit higher intensity values for the area (VII II) than for the other northern territories. The response of the alluvium-filled Taipei basin (with a depth of more than 400 m) may be considered as the reason for the phenomenon (Fletcher 2001).

During the Chi-Chi earthquake, some sites did show liquefaction, e.g., TCU110 and TCU065 (Wen and Yeh 2001). The recorded acceleration time histories are shown in Figure 14. The peak amplitudes for station TCU065 (N-S and E-W) are PGA 560 cm/s^2 and 770 cm/s^2; for station TCU110 (N-S and E-W)—PGA 188 cm/s^2 and 178 cm/s^2. The values of instrumental intensity for station TCU065 were calculated from spectra of horizontal components as 10.2 II and 10.1 II; for station TCU110—9.0 II and 8.9 II. The

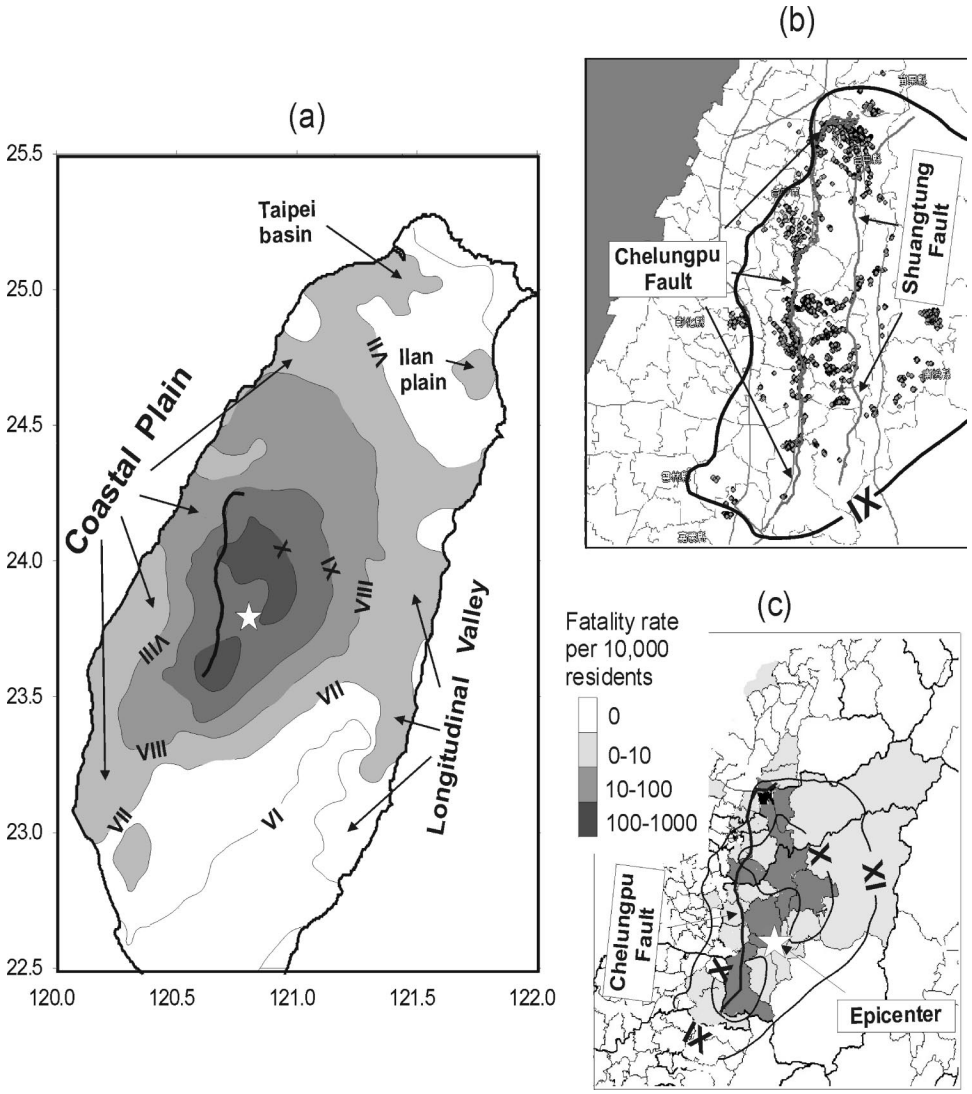

Figure 13. Instrumental intensity map for the Chi-Chi earthquake: (a) distribution of calculated intensity on the island, (b) epicentral area, symbols denote completely collapsed buildings (http://www.ncree.gov.tw), (c) comparison of theoretical isoseismals and fatality rate (after Y. B. Tsai, National Central University; see also http://www.ncree.gov.tw).

liquefaction phenomenon is one of the main reasons why buildings collapsed or were severely damaged during the earthquake, and the calculated intensity values reflect the severity of damage.

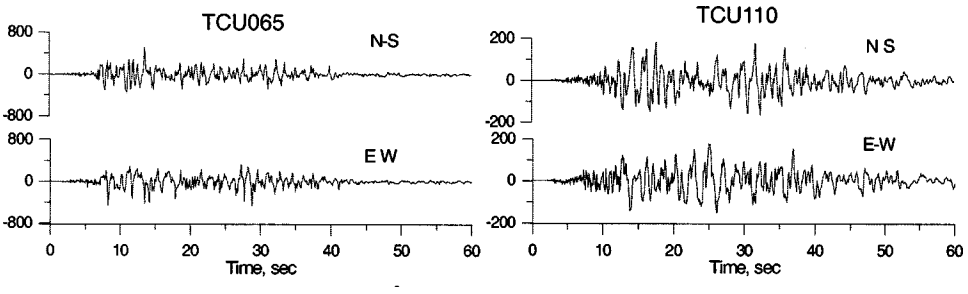

Figure 14. Acceleration records (cm/s^2) from stations located in liquefied area, the Chi-Chi earthquake main shock.

CONCLUSION

This paper presents the technique of seismic intensity (MMI or MSK scales) estimation on the basis of Fourier amplitude spectrum of ground acceleration. The method implies that seismic intensity depends on the level of spectra of ground acceleration. The relative contribution ("representativeness") of the spectral amplitudes at the considered frequencies (0.4-13 Hz) varies for different intensity levels. The most "representative" portions of the spectra (i.e., those that contribute the most to a particular seismic intensity) become wider and move to lower frequencies with increasing intensity. Therefore, as it has been shown in several studies (e.g., Chernov and Sokolov 1983, Aptikaev and Shebalin 1988, Chernov 1989, Wald et al. 1999c), when considering the relationship between the seismic intensity and characteristics of the observed ground motion, the intensity should correlate with ground acceleration for small intensities (less than MMI IV-V), ground velocity for intermediate intensities (MMI VI-VII), and ground vibrational displacement or residual displacement for large (more than MMI VIII) intensities.

The width of the frequency band, that is most "representative" for the given intensity value, should also be taken into account. It can be seen from Figure 5 that the width of the "most representative" frequency band (in this case it corresponds to the area of $\sigma_{1.3} \leqslant 1.3\sigma_{\mathrm{MIN}}$) increases from 0.5 units of $\log_{10} f$ for MMI V to 1.2 units of $\log_{10} f$ for MMI VIII. The intensity of MMI VIII implies the substantial damage of various constructions, buildings and their components, brittle and flexible, which are sensitive to various frequencies of vibration. The low intensities (MMI IV–V) are usually assigned on the basis of felt accounts that are associated with high-frequency vibrations. Thus, the high-amplitude, but narrow-band vibrations could produce strong resonance effects for a particular structure, however that vibration can hardly cause the overall damage, which should be assigned to high intensity level. The effect of the 1985 Michoacan (Mexico) earthquake in Mexico City is an example.

The use of Fourier amplitude spectra provides a natural consideration of site amplification by means of generalized or site-specific spectral ratios including those specified for large intensity motions and effect of soil nonlinearity. The site-specific amplification functions may be obtained on the basis of empirical records or numerical modeling that predicts the effect of alluvium-filled basins, very soft soils, or azimuthal differences in

the spectral amplification. Because the Fourier amplitude spectrum is a function of ground motion amplitude, frequency and duration, the shaking duration is also taken into consideration. The increase of duration leads to the higher spectral amplitudes and, therefore, to a higher intensity value. However, the relation between duration and intensity depends on the frequency of vibration and intensity level (Chernov 1989).

The established relationship between seismic intensity and Fourier amplitude spectrum seems to be region-independent, and the method may be used for the following purposes: (a) intensity pattern determination during future strong earthquakes on the basis of region- and site-dependent spectral models; (b) probabilistic seismic hazard assessment in terms of macroseismic intensity on regional (seismic zonation) and local (microzonation) scales (Sokolov 2000, Sokolov and Chernov 2001); and (c) early warning systems—rapid calculation of intensity maps on the basis of seismic network data.

Finally, it is necessary to note that the seismic intensity in terms of intensity scale is estimated using averaged data concerning the damage of different structures with different natural frequencies. Therefore the method described above (as well as other relationships between macroseismic intensity and ground motion parameters) can be applied only for estimation and prediction of "average" intensity without consideration of the behavior of any particular structure.

Obviously, there are several problems concerning some shortcomings of the described method. One of the major problems is the database extension for large (VIII-IX) intensities. The vertical components of the motion must be also taken into consideration. It seems to be useful also to introduce the magnitude/spectral amplitude relation especially for intermediate and small intensities (less than VII-VI MMI).

ACKNOWLEDGMENTS

The author is very grateful to D. Wald for conversations and valuable comments, and for providing the necessary data. The constructive suggestions from J. H. Steidl and anonymous reviewers allowed the author to improve the manuscript. M. Rizescu and K.-P. Bonjer provided the data for the Romanian events and J. Dewey provided the intensity data in digital form for some Californian earthquakes. Ground motion records of the Chi-Chi earthquake sequence were provided by Central Weather Bureau of the Republic of China. This study was carried out in the Collaborative Research Center (CRC) 461 "Strong Earthquakes: A Challenge for Geosciences and Civil Engineering," which is funded by the Deutsche Forschungsgemeinschaft (German Research Foundation) and supported by the state of Baden-Württemberg and the University of Karlsruhe.

REFERENCES

Ambraseys, N., Smit, P., Berardi, R., Rinaldis, D., Cotton, F., and Berge-Thierry, C., 2000. Dissemination of European Strong-Motion Data. CD-ROM collection. European Council, Environment and Climate Research Programme.

Aptikaev, F. F. and Shebalin, N. V., 1988. The correlation between macroseismic effects and dynamic parameters of ground motion, *Investigations of Seismic Hazard* (*Engineering Seismology Problems*, issue 29) (Nauka Publishing, Moscow), pp. 98–108 (in Russian).

Atkinson, G. M., and Silva, W., 2000. Stochastic modeling of California ground motions, *Bull. Seismol. Soc. Am.* **90**, 255–274.

Atkinson, G. M., and Sonley, E., 2000. Empirical relationships between Modified Mercalli Intensity and response spectra, *Bull. Seismol. Soc. Am.* **90**, 537–544.

Bakun, W. H., 1998. Modified Mercalli Intensities for some recent California earthquakes and historic San Francisco Bay region earthquakes, *U.S. Geol. Surv. Open-File Report 98–584*.

Bakun, W. H., 1999. Modified Mercalli Intensities for some California north coast earthquakes, *U.S. Geol. Surv. Open-File Report 99–171*.

Bendat, J. S., and Piersol, A. G., 1980. *Engineering Applications of Correlation and Spectral Analysis* (Wiley, New York).

Boore, D. M., and Atkinson, G. M., 1987. Stochastic prediction of ground motions and spectral response parameters at hard-rock sites in eastern North America, *Bull. Seismol. Soc. Am.* **77**, 440–467.

Boore, D. M., and Joyner, W. B., 1997. Site amplification for generic rock sites, *Bull. Seismol. Soc. Am.* **87**, 327–341.

Boatwright, J., Thywissen, K., and Seekins, L. C., 2001. Correlation of ground motion and intensity for the 17 January 1994 Northridge, California, earthquake, *Bull. Seismol. Soc. Am.* **91**, 739–752.

Building Seismic Safety Council (BSSC), 1995. *NEHRP Recommended Provisions for Seismic Regulations for New Buildings, 1994 Edition, Part I—Provisions, Part 2—Commentary*, developed for the Federal Emergency Management Agency, *FEMA 222* and *223*, Washington, DC.

Chen, C. C., Huang, C. T., Cheng, R. H., and Jeng, V., 2000. Preliminary investigation of damage to near-fault buildings of the 1999 Chi-Chi earthquake, *J. Earthquake Eng. Eng. Seismol.* **2**, 79–92.

Chernov, Yu. K., 1989. *Strong Ground Motion and Quantitative Assessment of Seismic Hazard* (Fan Publishing, Tashkent), 296 pp. (in Russian).

Chernov, Yu. K., and Sokolov, V. Yu., 1983. Relations between ground motion parameters and felt intensity, *Seismic Hazard Assessment* (*Engineering Seismology Problems*, issue 24) (Nauka Publishing, Moscow), pp. 96–111 (in Russian).

Chernov, Yu. K., and Sokolov, V. Yu., 1999. Correlation of seismic intensity with Fourier acceleration spectra, *Phys. Chem. Earth* **24** (6), 523–528.

Corsanego, A., 1995. Recent trends in the field of earthquake damage interpretation, *Proceedings of the 10th European Conference on Earthquake Engineering*, Balkema, Rotterdam, 763–771.

Denham, D., and Smith, W., 1993. Earthquake hazard assessment in the Australian Southwest Pacific Region: A review of the status quo, *Ann. Geofis.* **XXXVI**, N 3–4, pp. 27–39.

Dewey, J., 1997 (private communication).

Dowrick, D. J., Berryman, K. R., McVerry, G. H., and Zhao, J. H., 1998. Earthquake hazard in Christchurch, *New Zealand Nat. Soc. Earthquake Eng. Bull.* **31** (1), 1–23.

Fletcher, J. B., 2001. Ground motion in the Taipei and Ilan basins, *Seismol. Res. Lett.* **2**, 283.

Furumura, T., Koketsu, K., Wen, K. L., and Furumura, M., 2000. Numerical simulation of strong ground motion during the Chi-Chi, Taiwan, earthquake, *Proceedings of the International Workshop on the Annual Commemoration of the Chi-Chi Earthquake, September 18–20, 2000, NCREE*, Taipei, Taiwan, Vol. 1, pp. 222–232.

Irikura, K., Iwata, T., Sekiguchi, H., and Pitarka, A., 1996. Lessons from the 1995 Hyogo-Ken

Nanbu earthquake: Why were such destructive motions generated to buildings? *J. Nat. Disaster Sci.* **17** (2), 99–127.

Iwata, T., Sekiguchi, H., and Irikura, K., 2000. Rupture process of the 1999 Chi-Chi, Taiwan, earthquake and its near-source strong ground motions, *Proceedings of the International Workshop on the Annual Commemoration of the Chi-Chi Earthquake, September 18–20, 2000, NCREE, Taipei, Taiwan*, Vol. 1, 36–46.

Ji, C., Wald, D. J., and Helmberger, D. V., 2002. Source description of the 1999 Hector Mine, California, earthquake. Part II: complexity of slip history, *Bull. Seismol. Soc. Am.* **92** (in press).

Joyner, W. B. and Boore, D. M., 1986. On simulating large earthquakes by Green's-function addition of smaller earthquakes, *Proceedings of the Fifth Maurice Ewing Symposium on Earthquake Source Mechanics*, edited by S. Das, J. Boatwright, and C. Scholz, American Geophysical Union, pp. 269–274.

Krinitzsky, E. L., and Marcuson, W. F., 1983. Principles for selecting earthquake motions in engineering design, *Assn. Eng. Geolog., Bull.* **XX**, 253–265.

Lee, C. T., Kelson, K. I., and Kang, K. H., 2000. Hangingwall deformation and its effect to building and structures as learned from the Chelungpu faulting in the 1999 Chi-Chi Taiwan earthquake, *Proceedings of the International Workshop on the Annual Commemoration of the Chi-Chi Earthquake, September 18–20, 2000, NCREE, Taipei, Taiwan*, Vol. 1, pp. 93–104.

Lee, S. J., and Ma, K. F., 2000. Rupture process of the 1999 Chi-Chi, Taiwan, earthquake from the inversion of teleseismic data, *Terr. Atmos. Ocean Sci.* **11**, 591–608.

Murphy, J. R., and O'Brien, J. L., 1977. The correlation of peak ground acceleration amplitude with seismic intensity and other physical parameters, *Bull. Seismol. Soc. Am.* **67**, 877–915.

Ohta, Y., Kagami, H., Okada, S., and Ohashi, H., 1987. Seismic intensity and its application to engineering: a study in Japan, *Strong Ground Motion Seismology*, edited by M. O. Erdik and M. N. Toksoz (D. Reidel, Dordrecht), pp. 369–384.

Oncescu, M. C., Rizescu, M., and Bonjer, K.-P., 1992. Comparative study of accelerograms from 1986 and 1990 Vrancea earthquakes, *Report CEP/IFA 30.91.2*, Bucharest, 37 pp.

Oncescu, M. C., Bonjer, K.-P., and Rizescu, M., 1999. Weak and strong ground motion, source parameters and scaling laws for intermediate depth earthquakes from the Vrancea region, eastern Carpathians, *Vrancea Earthquakes: Tectonics, Hazard and Risk Mitigation*, edited by F. Wenzel, D. Lungu, and O. Novak (Kluwer, Dordrecht), pp. 27–42.

Park, S., and Elrick, S., 1998. Predictions of shear-wave velocities in Southern California using surface geology, *Bull. Seismol. Soc. Am.* **88**, 677–685.

Paz, M. (editor), 1994. *International Handbook of Earthquake Engineering, Codes, Programs, and Examples* (Chapman & Hall, New York).

Radu, C., and Polonic, G., 1979. Macroseismic field of the March 4, 1977 Vrancea earthquake, *Tectonophysics* **53**, 185–186.

Radu, C., Utale, A., and Winter, V., 1987. The August 30, 1986 Vrancea earthquake. Seismic intensity distribution, *National Institute for Earth Physics Report*, **II**, A-3.

Radu, C., and Utale, A., 1990. The May 30, 1990 Vrancea earthquake. Seismic intensity distribution, *Natl. Inst. Earth Phys. Rep.* **III**, A-4.

Raoof, M., Hermann, R., and Malagnini, L., 1999. Attenuation and excitation of three component ground motion in southern California, *Bull. Seismol. Soc. Am.* **89**, 888–902.

Savarenskii, E. F., 1975. *Seismic Waves* (Keter, Jerusalem).

Scientists from the U.S. Geological Survey, Southern California Earthquake Center, and Cali-

fornia Division of Mines and Geology, 2000. Preliminary report on the 16 October 1999 *M* 7.1 Hector Mine, California, earthquake, *Seismol. Res. Lett.* **71**, 11–23.

Shah, H., Boyle, R., and Dong, W., 1991. Geographic information systems and artificial intelligence. An application for seismic zonation, *Fourth International Conference on Seismic Zonation, Stanford, August 25–29, 1991, Proceedings*, Vol. I, pp. 487–517.

Schenk, V., Schenkova, Z., and Kottnauer, P., 1996. Earthquake hazard assessment for the Czech republic and adjacent area, *Earthquake Hazard and Risk*, edited by V. Schenk (Kluwer, Netherlands), pp. 125–140.

Slejko, D. and GNDT working group "Seismic Hazard," 1996. Preliminary seismic hazard assessment for the Italian seismic code, *Earthquake Hazard and Risk*, edited by V. Schenk (Kluwer, Netherlands), pp. 87–124.

Sokolov, V. Yu., 2000. Hazard-consistent ground motions: Generation on the basis of uniform hazard Fourier spectra, *Bull. Seismol. Soc. Am.* **90**, 1010–1027.

Sokolov, V. Yu., and Chernov, K. Yu., 1998. On the correlation of seismic intensity with Fourier amplitude spectra, *Earthquake Spectra* **14** (4), 679–694.

Sokolov, V. Yu., and Chernov, K. Yu., 2001. Probabilistic microzonation of urban territories: A case of Tashkent city, *Pure Appl. Geophys.* **158**, 2295–2311.

Spence, R., Coburn, A., and Pomonis, A., 1992. Correlation of ground motion with building damage: The definition of a new damage-based seismic intensity scale, *Proceedings of the Tenth World Conference on Earthquake Engineering, Madrid*, Vol. 1, 551–556.

Spence, R., Pomonis, A., Dowrick, D., and Cousins, W., 1998. Estimating human casualties in earthquakes: The case of Wellington, *Seismic Design Practice into the Next Century*, edited by E. Booth (Balkema, Rotterdam), pp. 277–286.

Trifunac, M. D., 1976. Preliminary empirical model for scaling Fourier amplitude spectra of strong ground acceleration in terms of Modified Mercalli Intensity and recording site conditions, *Earthquake Eng. Struct. Dyn.* **7**, 63–74.

Trifunac, M. D., 1989. Scaling strong motion Fourier spectra by Modified Mercalli Intensity, local soil and local geological site conditions, *Struct. Eng./Earthquake Eng.* **6**, 387–394.

Trifunac, M. D., and Brady, A. G., 1975. On the correlation of seismic intensity scales with the peaks of recorded strong ground motion, *Bull. Seismol. Soc. Am.* **65**, 139–162.

Trifunac, M. D., and Lee, V. W., 1985. Preliminary empirical model for scaling Fourier amplitude spectra of strong motion acceleration in terms of Modified Mercalli Intensity and geological site conditions, Department of Civil Engineering, *Report No. CE 85-04*, University Southern California, Los Angeles.

Trifunac, M. D., and Lee, V. W., 1989. Empirical models for scaling Fourier amplitude spectra of strong ground acceleration in terms of earthquake magnitude, source to station distance, site intensity and recording site conditions, *Int. J. Soil Dyn. Earthquake Eng.* **8**, 110–125.

Tsai, K. C., Hsiao, C. P., and Bruneau, M., 2000. Overview of building damages in 921 Chi-Chi earthquake *J. Earthquake Eng. Eng. Seismol.* **2**, 93–108.

Wald, D. J., Quitoriano, V., Dengler, L. A., and Dewey, J. W., 1999a. Utilization of the Internet for rapid community intensity maps, *Seismol. Res. Lett.* **70** (6), 680–697.

Wald, D. J., Quitoriano, V., Heaton, T. H., Kanamori, H., Scrivner, C. W., and Worden, C. B., 1999b. TriNet "ShakeMaps." Rapid generation of instrumental ground motion and intensity maps for earthquakes in southern California, *Earthquake Spectra* **15** (3), 537–555.

Wald, D. J., Quitoriano, V., Heaton, T. H., and Kanamori, H., 1999c. Relationships between peak

ground acceleration, peak ground velocity and Modified Mercalli Intensity in California, *Earthquake Spectra* **15** (3), 557–564.

Wang, H., 1995. The physical measure of seismic intensity, *Proceedings of the Fifth Conference on Seismic Zonation, Nice*, pp. 1189–1196.

Wen, K.-L., and Yeh, Y.-C., 2001. Nonlinear soil response during the 1999 Chi-Chi, Taiwan earthquake, *Seismol. Res. Lett.* **72**, 248.

Wills, C. J., Petersen, M. D., Bryant, W. A., Reichle, M. S., Saucedo, G. J., Tan, S. S., Taylor, G. C., and Treiman, J. A., 2000. A site conditions map for California based on geology and shear wave velocity, *Bull. Seismol. Soc. Am.* **90** (6B), 187–208.

Wu, M.-Y., Shin, T.-C., Chen, C.-C., Tsai, Y.-B., Lee, W., and Teng, T. L., 1997. Taiwan rapid earthquake information release system, *Seismol. Res. Lett.* **68**, 931–943.

Yong, C., Xinglian, C., Zhengxiang, F., Zhiqian, Y., and Mandong, Y., 1996. Estimating losses from future earthquakes in China, *Earthquake Hazard and Risk*, edited by V. Schenk (Kluwer, Netherlands), pp. 211–220.

(Received 17 February 2000; accepted 6 November 2001)